Dynamics of phase separation in a binary polymer blend of critical composition

Amitabha Chakrabarti
Department of Physics, Kansas State University, Manhattan, Kansas 66506[a] and Physics Department and Center for Polymer Science and Engineering, Lehigh University, Bethlehem, Pennsylvania 18015

Raul Toral
Physics Department and Center for Polymer Science and Engineering, Lehigh University, Bethlehem, Pennsylvania 18015 and Department de Fisica, Universitat de les Illes Balears, E-07071 Palma de Mallorca, Spain[a]

James D. Gunton
Physics Department and Center for Polymer Science and Engineering, Lehigh University, Bethlehem, Pennsylvania 18015

M. Muthukumar
Department of Polymer Science and Engineering, University of Massachusetts, Amherst, Massachusetts 01003

(Received 1 February 1990; accepted 26 February 1990)

We report results of a detailed numerical study of the phase separation process in a three dimensional model of polymer blends. The model system considered by us is described by Flory–Huggins–de Gennes free-energy functional. For a critical quench, we numerically integrate the corresponding time evolution equation for the conserved order parameter based on the above free-energy functional. We study the time dependence of the characteristic domain size as well as the pair correlation function and the structure factor for several quench temperatures. The results indicate that the growth law for the characteristic domain size is given by a modified Lifshitz–Slyozov law and the growth law exponent is *independent* of the quench temperature. We also find that both the pair correlation function and the structure factors show dynamical scaling at late times.

I. INTRODUCTION

The process of phase separation in a quenched system is the subject of many theoretical and experimental investigations in the field of small molecule or atomic systems, such as binary alloys, fluid mixtures, and inorganic glasses.[1] When such a system at the critical composition is quenched from a homogeneous, high temperature, phase to a point deep inside the coexistence curve (a critical quench), a small amplitude, long wavelength instability develops. This phenomenon is known as spinodal decomposition. At later times, the small inhomogeneities in the order parameter evolve into macroscopic domains of one or the other phase and an interconnected structure is formed. In recent years, the dynamics of spinodal decomposition in polymer blends have attracted much experimental[2–4] and theoretical[5–7] interest, since in these materials it is relatively easy to probe different regions of the phase diagram over widely varying time scales. The kinetics of phase separation in polymer blends is also unique in the sense that one needs to consider the collective movements of long-chain molecules in the process. Thus the important objectives in the study of phase separation in polymer mixtures are: (1) to look for *universality* in the dynamics of phase separation in general and (2) to discover possible *unique characteristics* originating from the presence of long-chain molecules in the system.

The theoretical understanding of the phase separation process in small molecule systems is based mainly on the Cahn–Hilliard–Cook (CHC)[8] formulation. The main ingredient of the CHC theory is a conserved field variable $\phi(\mathbf{x}, t)$ representing the local concentration of one of the components of the mixture (or, sometimes, the difference between the local concentration of the two components of a binary mixture). The time variation of this field is related to the functional derivative of a coarse-grained, free-energy functional $F[\phi]$ plus a thermal noise $\eta(\mathbf{x}, t)$ in the following way:

$$\frac{\partial\phi}{\partial t}=M\nabla^2\frac{\delta F}{\delta\phi}+\eta(\mathbf{x}, t), \tag{1}$$

where M is the mobility (assumed constant in theory) and the thermal noise η satisfies the fluctuation–dissipation theorem

$$\langle\eta(\mathbf{x}, t)\eta(\mathbf{x}', t')\rangle=-2k_BTM\nabla^2\delta(\mathbf{x}-\mathbf{x}')\delta(t-t') \tag{2}$$

in order to ensure approach to equilibrium at a temperature T. In this theory $F[\phi]$ is usually assumed to have the Ginzburg–Landau form $F_{GL}[\phi]$:

$$F_{GL}[\phi]=\frac{1}{2}\int d\mathbf{r}\left[-b\phi^2+\frac{u}{2}\phi^4+K|\nabla\phi|^2\right].$$

[a] Permanent address.

 0021-9606/90/116899-11$03.00

Analytical studies of this field-theoretic model have been reasonably successful in describing the early time regime[9–11] of the phase separation process, but, due to their approximate nature, they are not as useful in the so-called late stages. This late time regime is characterized by the coarsening of domains separated by interfaces whose thickness is much smaller than the characteristic domain size $R(t)$. The well known Lifshitz–Slyozov[12] theory, which predicts $R(t) = at^{1/3}$ at late times, is also not applicable as such for the spinodal decomposition process, since this theory is valid in the case of limitingly small volume fraction of one of the two phases. Attempts have been made to use renormalization group[13] and low-temperature perturbation methods[14] in order to study the late stages of evolution process for a critical quench. Numerical simulation also plays a useful role in our ability to understand and to predict the late time behavior of such a complicated system. Numerical studies[15,16] have suggested that the characteristic size of domains shows a modified[17] Lifshitz–Slyozov growth law ($R = a + bt^{1/3}$) and that the growth law exponent does not depend on the final temperature of quench,[16] as long as it is much smaller than the critical temperature of the system. Numerical studies also give strong support to the scaling ansatz, which states that at the late stages of phase separation process, there is only one length scale in the system, namely the characteristic size of the domains and hence the structure factor and the pair correlation functions should show dynamical scaling forms at late enough time.

Analytical studies of spinodal decomposition in polymer mixtures have been carried out by several authors[5–7] by using the CHC formulation with a Flory–Huggins–de Gennes free energy functional. Due to the same problems one faces in the study of small molecule systems, the calculations in polymer systems have dealt mainly with the early stages of the phase separation process as well. It seems, again, that numerical simulations can successfully probe the late time predictions of the theory that are inaccessible to analytical calculations. Monte Carlo simulation techniques have been used to study early stages of phase separation in a lattice model of polymer mixtures in two[18] and three dimensions.[19] In this paper, we discuss the results of a detailed numerical study of the CHC model in three dimensions starting from a full Flory–Huggins–de Gennes-type free-energy and numerically integrating the time evolution equation of the conserved order parameter up to sufficiently late time. A preliminary account of this study[20] has already been presented. This study is of particular interest since there is some controversy about the dynamical behavior observed in experiments with different polymer mixtures.[21–25] Recent experiments[21] on the phase separation of isotopic polymer mixtures have been interpreted to imply that (1) the growth law depends on the final temperature of quench and (2) the scaling behavior found in studies of small molecular systems does not seem to be valid for polymeric systems. The authors of this paper also suggested that the so-called "violation" of universal scaling is not observed in theoretical studies since these studies used with a Ginzburg–Landau-type free-energy, whereas the "true" free-energy functional for polymer mixtures is given by the Flory–Huggins–de Gennes expression. On the other hand, scaling was suggested to hold in several other experimental works on different polymer blends.[23–25] Since the different experiments do not agree with each other and there is no analytical theory valid at late times, we expect that the numerical simulation carried out by us will be useful in settling several important issues.

The main results of this study are the following. We find that the domain growth law for the model of polymer blends considered here is independent of the final temperature of quench and is consistent with the modified Lifshitz–Slyozov law.[17] In addition, the pair correlation function and the structure factor are shown to exhibit dynamical scaling at late enough times. The rest of the paper is organized as follows. In Sec. II, we describe the model and discuss the details of the numerical methods used. In Sec. III, we discuss the main results and finally we conclude in Sec. IV with a brief summary and concluding remarks.

II. MODEL AND NUMERICAL METHODS

A. Linear theory and definition of the rescaled variables

We consider a mixture of two polymer species, A, B, with chain lengths $N_A = N_B = N$ and subunit size $a_A = a_B = 1$. In order to study spinodal decomposition in polymer mixtures, we consider the concentration field $\varphi(\mathbf{x}, t)$ of one of the two polymers and choose for $F[\varphi]$ the full Flory–Huggins–de Gennes free energy given by[5–7]

$$\frac{F[\phi]}{k_BT} = \int d\mathbf{x}\left\{ f[\varphi(\mathbf{x})] + \frac{1}{36\varphi(1-\varphi)} |\nabla\varphi|^2 \right\}, \quad (4)$$

where

$$f[\varphi(\mathbf{x})] = \frac{1}{N}[\varphi \ln \varphi + (1-\varphi)\ln(1-\varphi)] + \chi\varphi(1-\varphi) \quad (5)$$

and χ is the temperature dependent Flory interaction parameter. The resulting equation after substituting expressions (4) and (5) into the general equation (1) is

$$\frac{\partial\varphi}{\partial t} = L(T)\nabla^2\left[\frac{1}{N}\ln\left(\frac{\varphi}{1-\varphi}\right) - 2\chi\varphi + \frac{1-2\varphi}{36\varphi^2(1-\varphi)^2}(\nabla\varphi)^2 - \frac{\nabla^2\varphi}{18\varphi(1-\varphi)}\right] + \eta(\mathbf{x}, t), \quad (6)$$

where we have defined $L(T) = MT$ and have set $k_B = 1$.

In the standard linearization approximation,[1,8] which is valid in the very early stages of the phase separation process, one writes $\phi(\mathbf{x}, t)$ as a sum of the average volume fraction ϕ_0($= 1/2$ in this case) and a small deviation $\delta\phi(\mathbf{x}, t)$ from the average, i.e.,

$$\phi(\mathbf{x}, t) = \phi_0 + \delta\phi(\mathbf{x}, t). \quad (7)$$

One then keeps only terms linear in $\delta\phi(\mathbf{x}, t)$ in the subsequent analysis. Linearizing Eq. (6) one finds

$$\frac{\partial \delta\phi(\mathbf{x},t)}{\partial t}=L(T)\nabla^2\left[\frac{4}{N}-2\chi-\frac{2}{9}\nabla^2\right]\delta\phi(\mathbf{x},t)+\eta(\mathbf{x},t). \tag{8}$$

Then in terms of the Fourier components $\delta\phi_{\mathbf{q}}(t)$ one writes Eq. (8) as

$$\frac{\partial \delta\phi_{\mathbf{q}}(t)}{\partial t}=-L(T)q^2\left[\frac{4}{N}-2\chi-\frac{2}{9}q^2\right]\delta\phi_{\mathbf{q}}(t)+\eta_{\mathbf{q}}(t), \tag{9}$$

where

$$\langle\eta_{\mathbf{q}}(t)\eta_{-\mathbf{q}}(t')\rangle=2L(T)q^2\delta(t-t'). \tag{10}$$

The structure factor of the system is defined as $S(q,t)=\langle|\phi_{\mathbf{q}}(t)|^2\rangle$ and can be written as

$$S(q,t)=S(q,0)e^{2R(q)t} \tag{11}$$

for early times. In Eq. (11) $R(q)$ is the amplification factor for wave vector q and is defined as

$$R(q)=-L(T)q^2\left[\frac{4}{N}-2\chi+\frac{2}{9}q^2\right]. \tag{12}$$

The linear theory predicts that fluctuations with wave vector $0<q<\sqrt{2}q_m^0$ become spontaneously amplified and grow exponentially. The wave vector q_m^0 at which the growth rate is maximum is defined by

$$\left.\frac{dR(q)}{dq}\right|_{q_m^0}=0 \tag{13}$$

and is given by

$$(q_m^0)^2=\frac{9}{2}(\chi-\chi_s), \tag{14}$$

where we have used $\chi_s=\chi(T=T_c)=2/N$. One can also define an apparent diffusion coefficient D_{app} in the framework of linear theory as

$$D_{\text{app}}=\left.\frac{R(q)}{q^2}\right|_{q^2=0}=2L(T)(\chi-\chi_s). \tag{15}$$

In experimental studies[3,21–25] one defines a rescaled wave vector k (in terms of the measured wave vector q) and a rescaled time τ as

$$k=q/q_m^0 \tag{16}$$

and

$$\tau=D_{\text{app}}(q_m^0)^2t. \tag{17}$$

In our numerical studies, we have used the slightly different rescaling: $k_1=q(\chi-\chi_s)^{-1/2}$ (correspondingly new space vector $\mathbf{x}_1=(\chi-\chi_s)^{1/2}\mathbf{x}$ in terms of the old space vector $\mathbf{x}$) and $\tau_1=2L(T)(\chi-\chi_s)^2t$. The relation between simulation and experimental variables is simply: $k_1=\sqrt{9/2}k$ and $\tau_1=2/9\tau$. Equation (6) becomes, in terms of these new reduced variables

$$\frac{\partial\varphi}{\partial\tau_1}=\frac{1}{2}\nabla^2\left[\frac{\chi_s}{2(\chi-\chi_s)}\ln\left(\frac{\varphi}{1-\varphi}\right)-\frac{2\chi}{\chi-\chi_s}\varphi+\frac{1-2\varphi}{36\varphi^2(1-\varphi)^2}(\nabla\varphi)^2-\frac{1}{18\varphi(1-\varphi)}\nabla^2\varphi\right]+\sqrt{\epsilon}\xi(\mathbf{x}_1,\tau_1), \tag{18}$$

where the new noise variable ξ satisfies

$$\langle\xi(\mathbf{x}_1,\tau_1)\xi(\mathbf{x}_1',\tau_1')\rangle=-\nabla^2\delta(\mathbf{x}_1-\mathbf{x}_1')\delta(\tau_1-\tau_1') \tag{19}$$

and $\epsilon=(\chi-\chi_s)^{1/2}$.

Numerically solving Eq. (18) in three dimensions is computationally a very demanding task. We have used a finite difference scheme for both the spatial and temporal derivatives. The spatial discretization is achieved by replacing the continuous space of position vectors by a simple cubic lattice $N=L^3$ sites and lattice spacing (mesh size) Δr. We numerically integrate Eq. (18) by using a first order Euler scheme,

$$\phi(\mathbf{x}_1,\tau_1+\Delta\tau_1)=\phi(\mathbf{x}_1,\tau_1)+\Delta\tau_1\frac{\partial\phi}{\partial\tau_1} \tag{20}$$

with a time step $\Delta\tau_1$. In order to carry out the calculations within a reasonable amount of computer time one would like to choose a large time step and a moderately large system size. However, the discretized version of Eq. (18) develops numerical instability for large time steps. We have used a time step of $\Delta\tau_1=0.01$ to integrate Eq. (18). We find that the numerical integration is stable for this value of $\Delta\tau_1$ and smaller values of $\Delta\tau_1$ do not change quantities that express a global behavior, such as the structure function, the pair correlation function or the typical domain size. For the polybutadiene system studied in recent experiments,[21,22] the critical temperature and the χ parameter are known[26] and these values are used as the input for the numerical studies. Thus by varying χ one can faithfully mimic the quench procedure at different final temperatures. We have taken $\chi=0.326/T-2.3\times10^{-4}$, $T_c=62\,^{\circ}\text{C}$ and the quench temperatures 25, 40, 49, and 54.5 °C. With these input parameters, we have numerically integrated Eq. (18) on a simple cubic lattice of size 50^3 with periodic boundary conditions and mesh size $\Delta r=1$. We have performed the numerical integration up to $\tau_1=500$ (corresponding to $\tau=2250$) for quench temperatures 25 and 49 °C, whereas the integrations are carried out to $\tau_1=50$ (correspondingly $\tau=225$) for quench temperatures 40 and 54.5 °C. We have always started with the initial configuration $\phi=\frac{1}{2}$ everywhere and in order to average over the noise, we have performed 20 runs for each quench temperature. Although we have used rescaled variable x_1 and τ_1 in Eq. (18), in the following sections, we report our results in terms of the rescaled variable k and τ used in the experimental studies for direct comparison. The corresponding rescaled space vector is defined as $\mathbf{r}=\mathbf{x}q_m^0$.

B. Computation of different probes

Dynamical scaling and growth laws for the average domain size have been traditionally analyzed in terms of the structure function

$$S(\mathbf{k},\tau)=\left\langle\frac{1}{N}\sum_{r}\sum_{r'}e^{i\mathbf{k}\mathbf{r}}[\phi(\mathbf{r}+\mathbf{r}',\tau)\phi(\mathbf{r}',\tau)-\langle\phi\rangle^2]\right\rangle, \tag{21}$$

where the sum runs over the lattice and the k vectors belong to the first Brillouin zone in the reciprocal space, i.e., $\mathbf{k} = (2\pi/L\Delta r)\mu$, $\mu\equiv(\mu_x,\mu_y,\mu_z)$, and $0 \leqslant \mu_x,\mu_y,\mu_{bf} \leqslant l-1$. We then define a spherically averaged structure factor as

$$S(k,t)=\sum_{k-(\Delta k/2)<|k|<k+(\Delta k/2)} S(k,\tau)/n(k,\Delta k), \tag{22}$$

where

$$n(k,\Delta k)=\sum_{k-(\Delta k/2)>|k|<k+(\Delta k/2)} 1. \tag{23}$$

The quantity defined in Eq. (23) denotes the number of lattice points in a spherical shell of width Δk centered around k. Ideally, one should take Δk as small as possible. A convenient value for the discretized Brillouin zone considered in the simulation, though, is $\Delta k = \frac{2\pi}{L\Delta r}$. Our results for $S(k,\tau)$ for various τ are shown in Fig. 1 for quench temperature 25 °C.

For typical measures of domain size, one usually considers either the location $k_m(\tau)$ of the peak of the spherically averaged structure factor or some moment of $S(k,\tau)$. We have calculated the location of the peak $k_m(\tau)$ in the following way. For different values of τ, we have fitted the three points near the maximum of $S(k,\tau)$ to a parabolic form and calculated $k_m(\tau)$ and $S_m(\tau) = S(k_m,\tau)$ from the maximum of this fitted function.

In recent years, scaling and growth laws have also been analyzed in terms of the real-space correlation function $G(\mathbf{r},\tau)$ defined as

$$G(\mathbf{r},\tau)=\sum_{\mathbf{k}} e^{i\mathbf{k}\cdot\mathbf{r}}S(k,\tau). \tag{24}$$

In this case also we perform a spherical average procedure as described above and obtain the corresponding correlation function $G(r,\tau)$. We then define a normalized correlation function $g(r,\tau)$ defined as

$$g(r,\tau)=G(r,\tau)/G(r,0) \tag{25}$$

such that $g(0,\tau) = 1$. The domain morphology for the conserved order parameter produces a damped oscillatory behavior in $g(r,\tau)$ (Fig. 2). This allows one to give a quantitative measure of the domain size (R_g) as the location of the first zero of the correlation function. The length R_g was calculated fitting the four points in $g(r,\tau)$ closest to its first zero (of which two fall on each side of its first zero) to a cubic polynomial of r and defining R_g as the value of r where this fitted function vanishes.

III. RESULTS

A. Growth law

In several experimental studies,[3,25] when the rescaled wave vector $k_m(\tau)$ is plotted against the rescaled time τ, one observes that the data for several different quench temperatures fall on a universal curve, thus indicating that the domain growth law is independent of the quench temperature. However, as mentioned earlier, results of recent experiments on isotopic polymer blends[21,22] suggest a

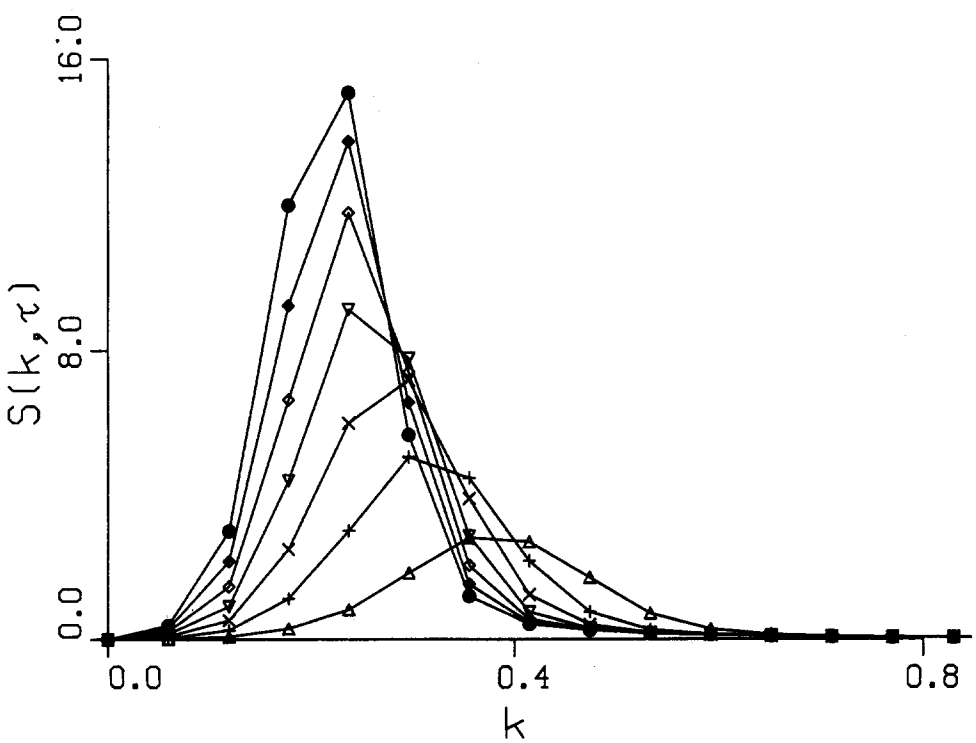

FIG. 1. The spherically averaged structure factor $S(k,\tau)$ vs k for several values of τ for quench temperature 25 °C. The symbols are as follows: △ (τ = 225), + (τ = 450), × (τ = 675), ▽ (τ = 900), ◇ (τ = 1125), ◈ (τ = 1350) and ● (τ = 1575).

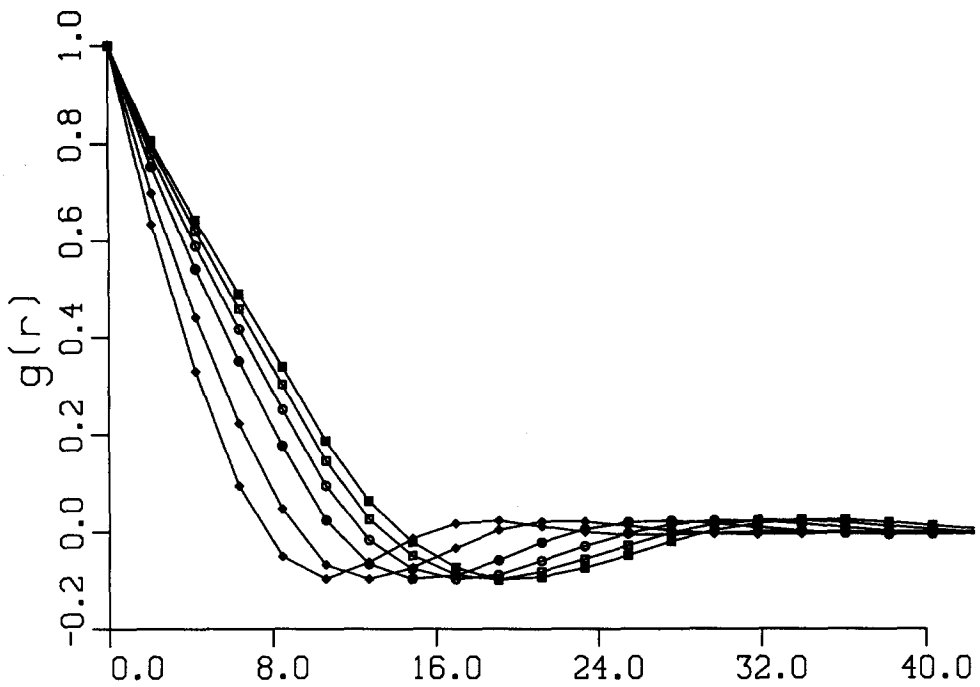

FIG. 2. The spherically averaged pair correlation function $g(r, t)$ vs r for several values of τ for $T = 25$ °C. The symbols are as follows: ◇ ($\tau = 225$), ◆ ($\tau = 450$), ● ($\tau = 900$), ○ ($\tau = 1350$), □ ($\tau = 1800$), and ■ ($\tau = 2250$).

quench-depth dependent growth law. Our results for $\ln k_m$ vs $\ln \tau$ and $\ln R_g$ vs $\ln \tau$ are plotted in Fig. 3(a) and Fig. 3(b), respectively, for several values of the quench temperature. The determination of k_m is less reliable than that of R_g, because k_m is computed by locating the maximum of the structure function, which particularly at late times, is not precisely defined (see Fig. 1) due to the discretization of the Brillouin zone in a finite lattice such as considered here. This explains the small bends in the $\ln k_m$ vs $\ln \tau$ curves for, say, $\tau > 500$ in Fig. 3(a). Another source of error is the statistical fluctuation of data coming from different runs. For the domain size measures, the statistical errors are of the order of a few percents.

In Figs. 3(a) and 3(b) we see that the growth law exponent is independent of the quench temperature. This result is consistent with the claimed universal scaling of Refs. 3 and 25, but not with that of Ref. 21, where a quench-depth dependent growth law exponent is suggested for early to intermediate stages. The growth law exponent calculated from the slope of these log–log plots is given by 0.28 ± 0.01. This value of the growth exponent is in excellent agreement with the experimental result for intermediate to "transition" times.[22] We point out that the physical mechanism governing the late time behavior in the model corresponds to the so-called "transition" times in experimental systems, whereas the "real" late time behavior seen in the experiments is governed by hydrodynamic interactions.[27,28] We also find that the peak of the structure factor $S_m(\tau)$ yields an effective growth law exponent of 0.85 ± 0.02 (Fig. 4), also in good agreement with recent experiments.[22]

We point out that the exponents found from the log–log plots are probably effective exponents, since one expects[17] that the growth law for domain size $R(\tau)$ is given by $R(\tau) = a + b\tau^n$. A fit to this expression of the R_g data between $\tau = 450$ and $\tau = 2250$ yields $n = 0.33 \pm 0.01$ for $T = 25$ °C and $n = 0.33 \pm 0.02$ for $T = 49$ °C. This value of the exponent suggests that the Lifshitz-Slyozov mechanism describes the growth of domains in this time regime.

B. Scaling

The late stages of the dynamical process can be described in terms of an asymptotic scaling with a time dependent length. The fundamental assumption is that in the asymptotic scaling regime only one length $R(\tau)$ is relevant. This length $R(\tau)$ represents the characteristic size of the domains. Then the dynamical scaling hypothesis states that

$$g(r, \tau) = \mathbf{G}[r/R(\tau)] \tag{26}$$

and, consequently

$$S(k, \tau) = R(\tau)^d \mathbf{F}[kR(t)], \tag{27}$$

where both $\mathbf{G}(\rho)$ and $\mathbf{F}(X)$ are time independent functions.

Figure 5(a) and 5(b) show the scaling behavior of $g(r, \tau)$ with R_g as the scaling length for $T = 25$ °C and $T = 49$ °C, respectively. The scaling hypothesis [Eq. (26)] seems to be well satisfied, over the whole range of values of r considered here, particularly at late times. However, scaling can not be checked for arbitrary large values of the scaling variable ρ due to the finiteness of the system.

The scaling ansatz, Eq. (27) can be tested by plotting $S(k, \tau) k_m(\tau)^3$ vs $X = k/k_m(\tau)$ and checking whether the

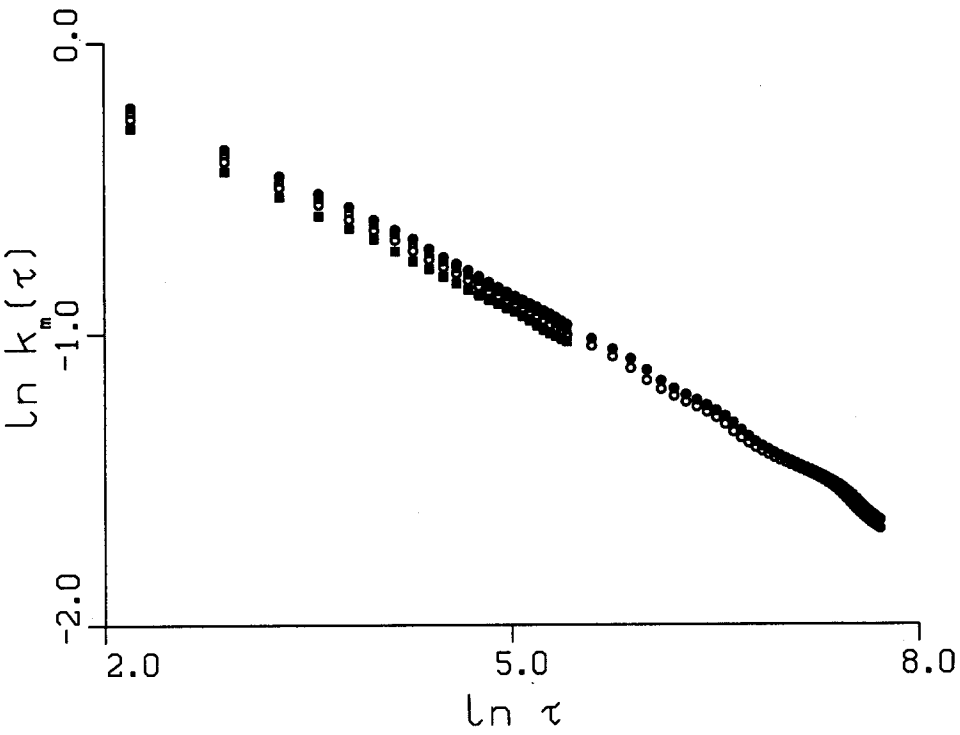

FIG. 3. (a). The location of the maximum of the structure factor k_m vs τ shown in log–log scale for several quench temperatures. The growth law exponent (0.28 ± 0.01), computed for $50 < \tau < 1000$ is independent of the quench temperature. (b). The characteristic domain size R_g calculated from the pair correlation function (see the text) plotted against rescaled time τ for several quench temperatures. The qualitative behavior is same as in (a).

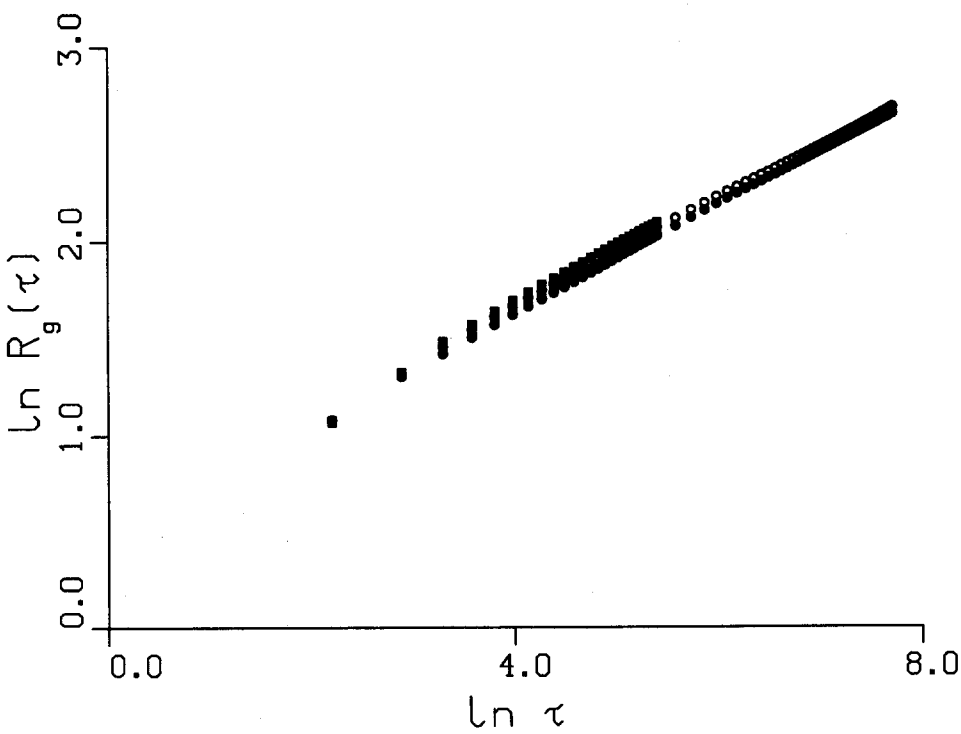

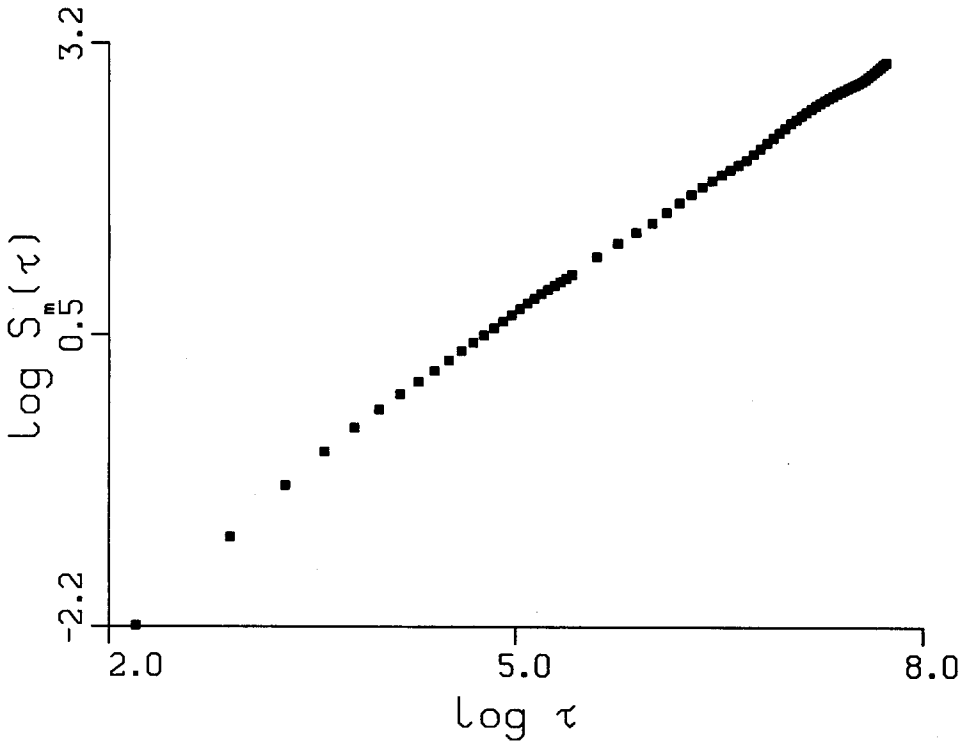

FIG. 4. The maximum of the structure factor S_m vs τ shown in log–log scale for quench temperature $T = 25$ °C. The growth law exponent for $S_m(0.85 \pm 0.02)$, computed for $50 < \tau < 1000$ is also found to be independent of the quench temperature.

resulting functions are independent of time. In Figs. 6(a) and 6(b) we show such plots for late times. It is clear from these figures that dynamical scaling is well satisfied for large times τ. Scaling is not totally satisfactory near the peak due to the uncertainty in locating the maximum of the structure factor at late times, as discussed earlier. Since we believe that the computation of R_g is more reliable at late times, we also show the scaling plot of $S(k, \tau)/R_g(\tau)^3$ vs $kR_g(\tau)$ in Fig. 6(c) for the quench temperature 25 °C. By comparing this plot with that of Fig. 6(a) it seems that this scaling plot is relatively smoother than that with $k_m(\tau)$ as the scaling variable.

In order to study the functional form of the scaling curve, we plot the structure factor data for both $T = 25$ °C and $T = 49$ °C in log–log graphs in Figs. 7(a) and 7(b), respectively. It is again clear from this figure that the scaling hypothesis works at late times where all the curves fall on top of each other. It is interesting to note that the scaling function exhibits a weak shoulder around $k \approx 2k_m(\tau)$ which has also been observed in the most recent experimental systems[22,24] and predicted in some theoretical calculations[29] as well. The straight lines in Figs. 7(a) and 7(b) are the fit to the data for large k values for each quench temperature. We find that for large k, the scaling function goes as $k^{-3.6}$, which is close to the expected Porod's law behavior (k^{-4}). In recent experimental studies[22,24] it has also been found that for late times the scaling function behaves as k^{-4} for large k. In order to compare the scaling functions with the phenomenological expression for the scaling function introduced by Furukawa,[30,31] we suitably rescale the axes of the scaling functions [such that the maximum of the scaling function is located at (1,1)] and compare with the Furukawa functions

$$F(X) = \frac{4X^2}{3 + X^8} \tag{28}$$

and

$$F(X) = \frac{3X^3}{2 + X^9} \tag{29}$$

in Fig. 8. It is clear that neither of Furukawa's forms agrees with our data over the whole range of k values.

IV. CONCLUDING REMARKS

In this paper we have presented detailed numerical studies of a complicated stochastic nonlinear partial differential equation appropriate for modeling the dynamics of phase separation and pattern formation in polymer blends. An accurate solution of this equation requires the introduction of a space discretization with a very large number of lattice points and a relatively small time step. Also, in order to confirm theoretical ansatzs concerning the scaling behavior of the system, it is necessary to solve the equation up to a very late time. Finally, the stochastic nature of the equations requires an average over many realizations. Thus, this problem belongs to the category of those needing an extensive use of the resources (both memory and CPU) of powerful supercomputers. We have focused mainly on the late time behavior for a reasonably large

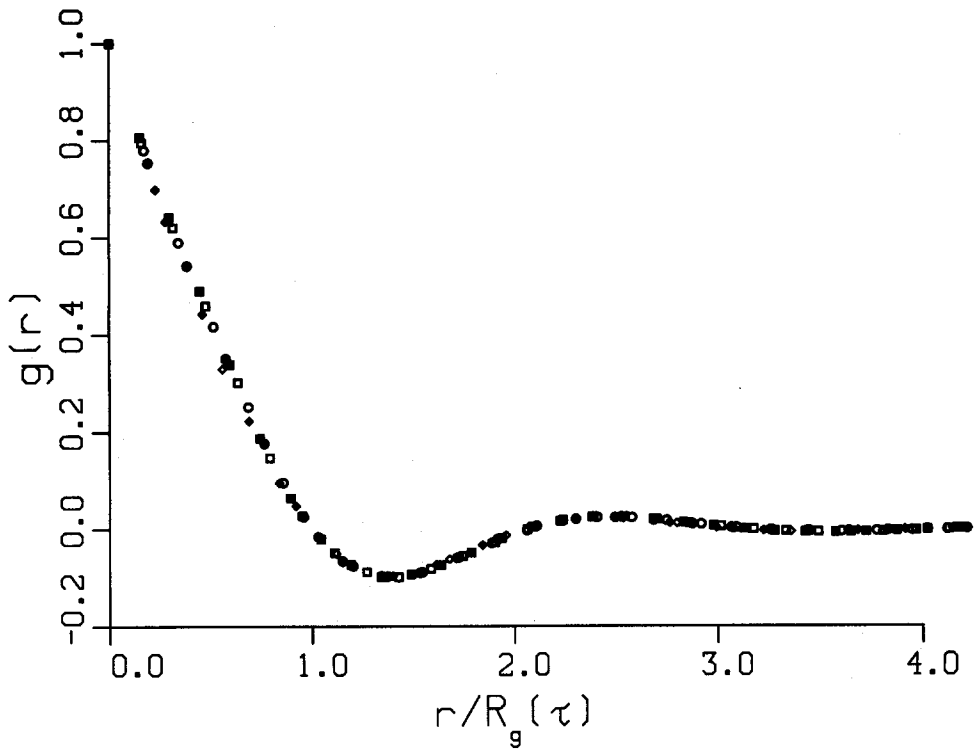

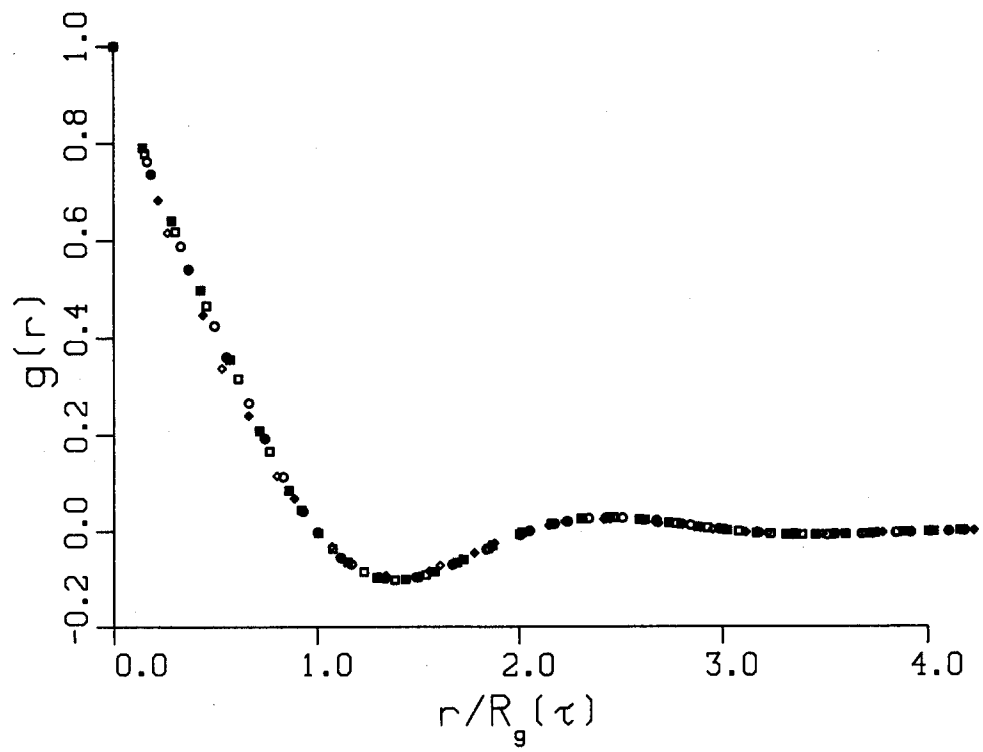

FIG. 5. (a). Plot of the scaling function defined in Eq. (26) for the spherically averaged and normalized pair correlation function for quench temperature 25 °C. The symbols have the same meaning as in Fig. 2. Scaling is well satisfied at late times. (b) Plot of the scaling function defined in Eq. (26) for the spherically averaged and normalized pair correlation function for quench temperature 49 °C. The symbols have the same meaning as in Fig. 2. Scaling is well satisfied at late times.

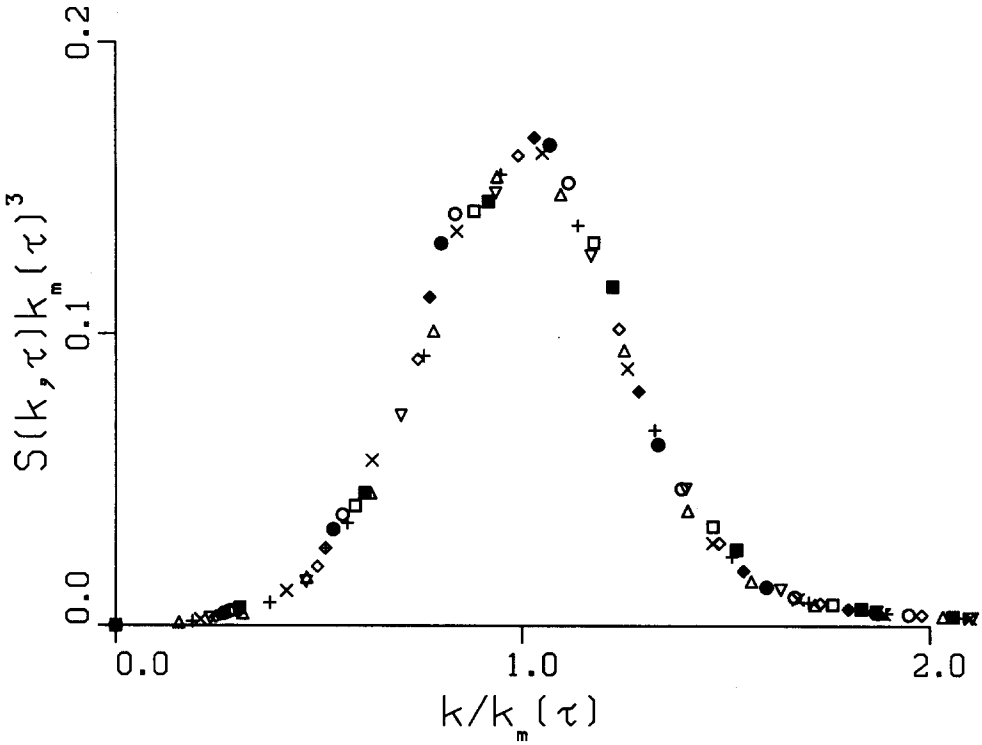

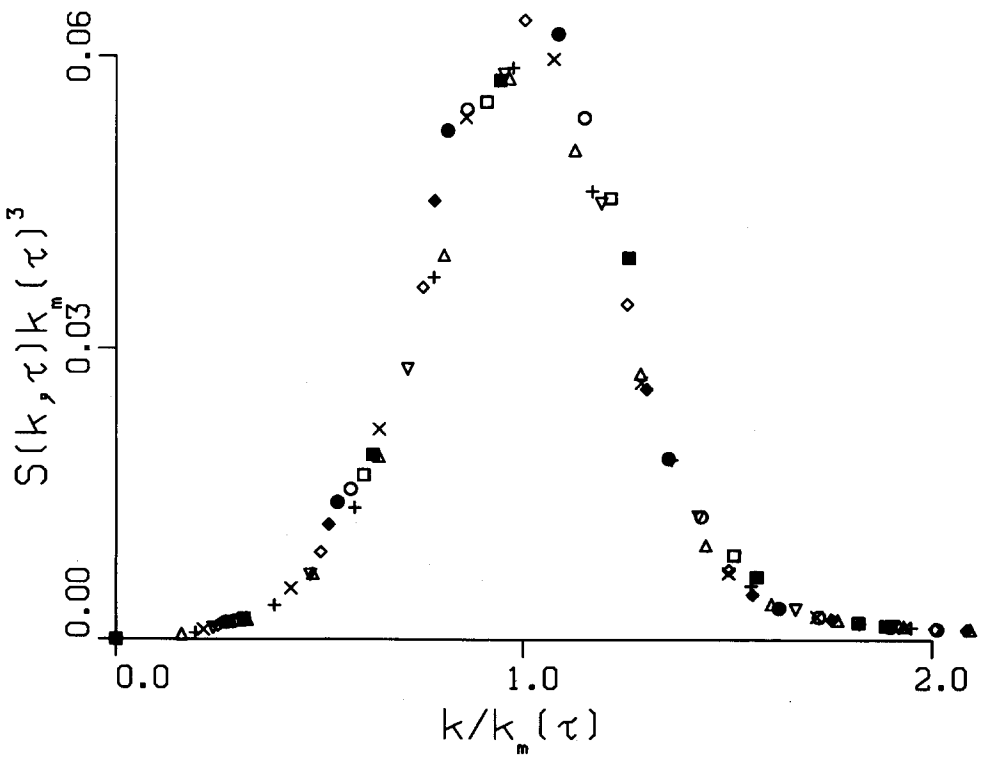

FIG. 6. (a) Plot of the scaling function defined in Eq. (25) for spherically averaged structure factor with k_m^{-1} as the scaling length and for quench temperature 25 °C for several values of τ. The symbols are as follows: △ (τ = 225), + (τ = 450), × (τ = 675), ▽ (τ = 900), ◇ (τ = 1125), ◈ (τ = 1350), ● (τ = 1575),(τ = 1800), □ (τ = 2025), and ■ (τ = 2250). (b) Plot of the scaling function defined in Eq. (25) for spherically averaged structure factor with k_m^{-1} as the scaling length and for quench temperature 49 °C for several values of τ. The symbols are the same as in (a).

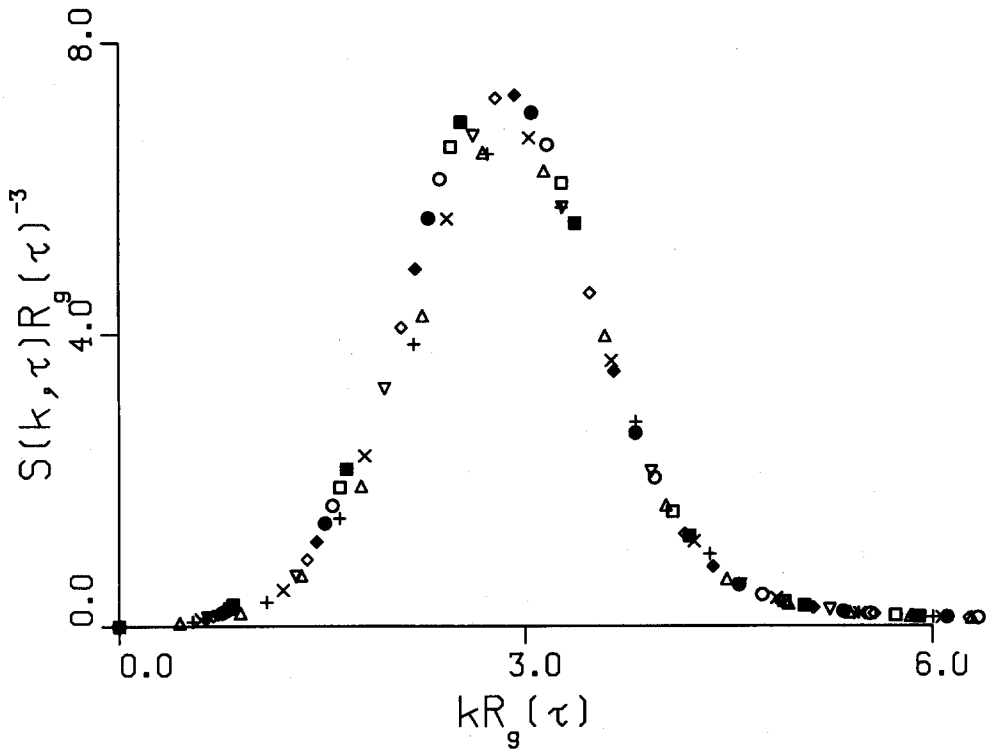

FIG. 6(c). Plot of the scaling function defined in Eq. (25) for spherically averaged structure factor with R_g as the scaling length and for quench temperature 25 °C for several values of τ. The symbols are the same as in (a). The vertical axis is multiplied by 10^3.

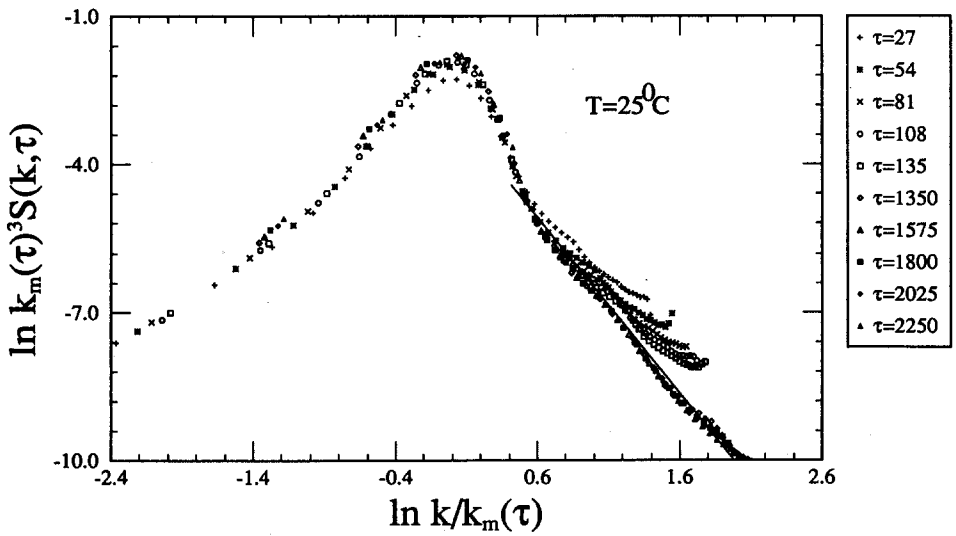

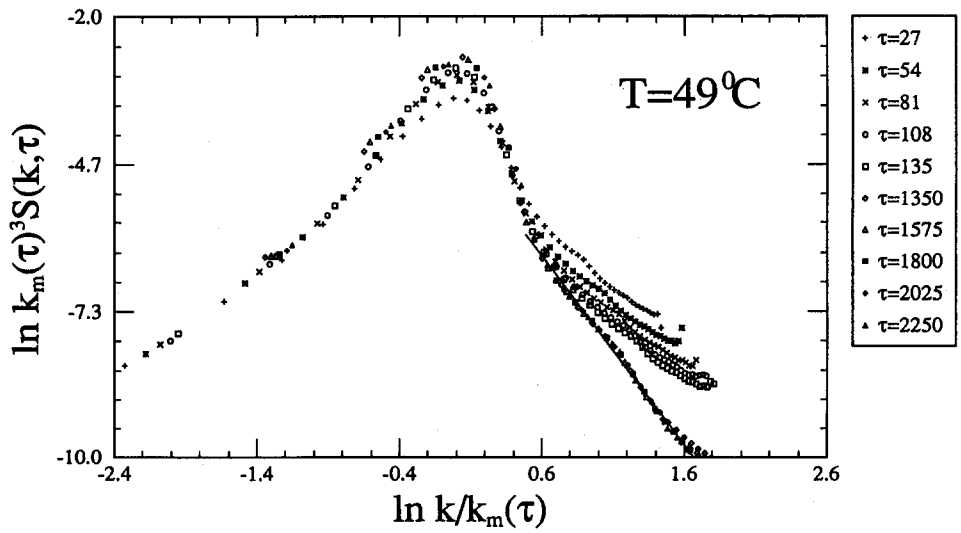

FIG. 7. (a) Plot of the scaling function [as in Fig. 6(a)] in log–log scale. The straight line is a fit to the data for large k, with a slope of -3.6. (b) Plot of the scaling function [as in Fig. 6(b)] in log–log scale. The straight line is a fit to the data for large k, with a slope of -3.6.

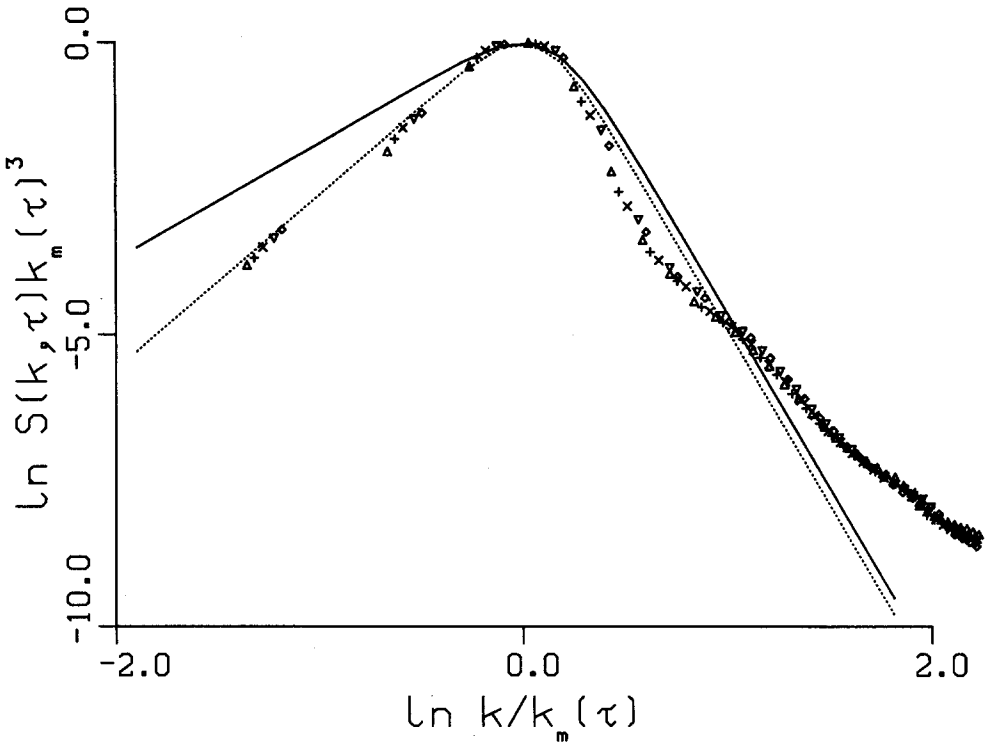

FIG. 8. Plot of the normalized scaling function for the structure function for quench temperature 25 °C (see the text) in a log–log scale. The solid and the dotted lines are the predictions of Eqs. (28) and (29), respectively.

system, in the absence of hydrodynamic interactions. We find that, at sufficiently late times, the scattering intensity and the pair correlation functions are well represented in terms of scaling with a time dependent length. Our analysis of the time dependence of this characteristic length supports a modified Lifshitz–Slyozov law in which the asymptotic growth law exponent is 1/3. We also found that the growth law is independent of the final quench temperature.

Finally, we mention future directions in which we are extending our works. As mentioned earlier, recent experiments on polymer blends indicate that the growth law for the average domain size depends on the final temperature of quench. We do not see such a temperature dependent growth law in our studies. However, in real polymer mixtures, the Onsager coefficient is wave vector dependent,[5,7] as well as the χ parameter depends on composition.[32] We plan to address these questions in future studies.

ACKNOWLEDGMENTS

This work was supported by NSF Grant No. DMR-8612609 and DMR-8420962 and by an NSF grant of computer time at the Pittsburgh Supercomputing Center. R. T. acknowledges financial support from DGICYT Project No. PB-86-0534 (Spain).

[1] For a review, see J. D. Gunton, M. San Miguel, and P. S. Sahni, in *Phase Transitions and Critical Phenomena*, edited by C. Domb and J. L. Lebowitz (Academic, London, 1983), Vol. 8.
[2] T. Hashimoto, in *Current Topics in Polymer Science*, Vol. II, edited by R. M. Ottenbrite, L. A. Utracki, and S. Inoue (Hanser, Munich, 1987).
[3] T. Hashimoto, Phase Transitions, **12**, 47 (1988).
[4] T. Nose, Phase Transitions **8**, 245 (1987).
[5] P. G. de Gennes, J. Chem. Phys. **72**, 4756 (1980).
[6] P. Pincus, J. Chem. Phys. **75**, 1996 (1981).
[7] K. Binder, J. Chem. Phys. **79**, 6387 (1983).
[8] J. W. Cahn and J. E. Hilliard, J. Chem. Phys. **28**, 258 (1958); H. E. Cook, Acta Metall. **18**, 297 (1970).
[9] J. S. Langer, Ann. Phys. **65**, 53 (1971).
[10] J. S. Langer, M. Baron, and H. D. Miller, Phys. Rev. A **11**, 1417 (1975).
[11] M. Grant, M. San Miguel, J. Viñals, and J. D. Gunton, Phys. Rev. B **31**, 3027 (1985).
[12] I. M. Lifshitz and V. V. Slyozov, J. Phys. Chem. Solids **19**, 35 (1961).
[13] A. J. Bray, Phys. Rev. Lett. **62**, 2841 (1989); *ibid.* **63**, 818 (E) (1989).
[14] G. F. Mazenko, Phys. Rev. Lett. **63**, 1605 (1989) and references therein.
[15] R. Toral, A. Chakrabarti, and J. D. Gunton. Phys. Rev. Lett. **60**, 2311 (1988); A. Chakrabarti, R. Toral, and J. D. Gunton, Phys. Rev. B **39**, 4386 (1989).
[16] J. G. Amar, F. E. Sullivan, and R. D. Mountain. Phys. Rev. B **37**, 196 (1988); T. M. Rogers, K. R. Elder, and R. C. Desai, *ibid.* B **37**, 9638 (1988); E. T. Gawlinski, J. D. Gunton and J. Viñals, *ibid.* **39**, 7266 (1989).
[17] D. A. Huse, Phys. Rev. B **34**, 7845 (1986).
[18] A. Baumgartner and D. W. Heermann, Polymer **27**, 1777 (1986).
[19] A. Sariban and K. Binder, Pol. Commun. **30**, 205 (1989).
[20] A. Chakrabarti, R. Toral, J. D. Gunton, and M. Muthukumar, Phys. Rev. Lett. **63**, 2072 (1989).
[21] P. Wiltzius, F. S. Bates, and W. R. Heffner, Phys. Rev. Lett. **60**, 1538 (1988).
[22] F. S. Bates and P. Wiltzius, J. Chem. Phys. **91**, 3258 (1989).
[23] T. Hashimoto, in *Dynamics of Ordering Process in Condensed Matter*, edited by S. Komura (Plenum, New York, 1988).
[24] T. Hashimoto, M. Takenaka, and T. Izumitani, Pol. Commun. **30**, 45 (1989).
[25] H. L. Snyder and P. Meakin, J. Chem. Phys. **79**, 5588 (1983).
[26] F. S. Bates, G. D. Wignall and W. C. Koehler, Phys. Rev. Lett. **55**, 2425 (1985).
[27] E. D. Siggia, Phys. Rev. A **20**, 595 (1979).
[28] A. Onuki, J. Chem. Phys. **85**, 1122 (1986).
[29] T. Ohta and H. Nozaki (preprint).
[30] H. Furukawa, Physica, A **123**, 497 (1984).
[31] H. Furukawa, Phys. Rev. B **33**, 638 (1986).
[32] F. S. Bates, M. Muthukumar, G. D. Wignall, and L. J. Fetters, J. Chem. Phys. **89**, 535 (1989).